

Fabrication of collagen immobilized electrospun poly (vinyl alcohol) scaffolds

Burcu Oktay^a, Nilhan Kayaman-Apohan^{a*}, Serap Erdem-Kuruca^b and Mediha Süleymanoğlu^b



In the development of tissue engineering scaffolds, the interactions between material surface and cells play crucial roles. The biomimetic 3-D scaffolds absolutely provide better results for fulfilling requirements such as porosity, interconnectivity, cell attachment and proliferation. In this study, 3-D electrospun scaffolds were prepared by using an electrospinning technique. Photo cross-linkable polyvinyl alcohol was used as a polymeric matrix. During the electrospinning, the nanofibers were cross-linked with *in situ* ultraviolet radiation. The crosslinked polymer fibers were achieved in a simple process at a single step. Nanofiber surface was modified with collagen by a chemical approach. The chemical structures were proven by attenuated total reflectance Fourier transform infrared spectroscopy and proton nuclear magnetic resonance. The surface morphology of the nanofibers was characterized by scanning electron microscope (SEM). Morphological investigations show that the resulting nanofibrous matrix has uniform morphology with a diameter of 220–250 nm. *In vitro* attachment and growth of 3T3 mouse fibroblasts and human umbilical vein endothelial cells (ECV304) cells on polyvinyl alcohol-based nanofiber mats were also investigated. Cell attachment, proliferation, and methylthiazole tetrazolium cytotoxicity assays indicated good cell viability throughout the culture time, which was also confirmed by SEM analysis. Copyright © 2015 John Wiley & Sons, Ltd.

Supporting information may be found in the online version of this paper.

Keywords: electrospinning; nanofiber; methacrylated polyvinyl alcohol; electrospun scaffold; collagen

INTRODUCTION

Tissues of the human body are composed of two main components: cells and extracellular matrix (ECM). ECM provides structural support to the surrounding cells and regulates intercellular communication.^[1] Tissue engineering is a multidisciplinary field that focuses on the replacement, repair, maintenance, and/or enhancement of tissue function. In the past decade, the synthetic and natural polymers have been effectively used to create bioactive ECM analogues scaffolds.^[2,3] An ideal tissue engineering scaffold should mimic both the form and functionality of the native ECM. Besides, they should possess high porosity and uniform pore size.^[4] The porous polymer scaffolds can be created using various fabrication techniques such as salt leaching, phase separation, emulsion templating, and electrospinning. Electrospinning is a versatile and easy technique for preparing nanofiber mats. The principle and theory of electrospinning have been described in literature.^[5–8] For electrospinning, little specialized equipment is required and all that is needed is a high voltage power source, a collector, and a small diameter conductive capillary. The resulting nanofiber mats have large surface area to volume ratio, large porosity, and flexibility.^[9] The 3-D nanofiber matrix tends to promote cells spreading and proliferation because it is similar to the fibrous structure of native ECM. Several studies have been published about nanofiber and their applicability to tissue engineering. Cai *et al.* prepared 3D and two 2D electrospun scaffolds. It is observed that the cells have remarkably better attachment, proliferation, and penetration showed onto 3-D scaffold compared with 2-D scaffold.^[10] In another study, Jue *et al.* developed a novel sandwich model for fabrication of delicate 3-D structures in

cartilage engineering. A thin layer of gelatin-polycaprolactone (GT-PCL) electrospun scaffold was used as a carrier. The chondrocytes were seeded on the membranes. Another GT-PCL membrane was stacked on top of the layer by seeding the same number of cells. *In vitro* and *in vivo* cultivations were performed. The results demonstrate that the engineering of 3-D cartilage structure in a sandwich model using electrospun membranes is an effective approach.^[11] Collagen is a natural polymer, which can help to imitate structure of extracellular matrix. Collagen type I accounts for up to 70–90% of the collagen found in many tissue types, but is mainly associated with tissues, such as tendons and ligaments. Indeed, collagen has a triple helical structure.^[12,13] Kawalec *et al.* reported the preparation of poly[(R,S)-3-hydroxybutyrate] (aPHB)/poly[(R)-3-hydroxybutyrate] (PHB) (85/15 w/w) blend scaffolds by electrospinning. Human procollagen type I was immersed on the scaffold. After the modification with collagen, biocompatibility of the final scaffolds significantly increased. Based on these findings, collagen-modified aPHB/PHB scaffolds can be considered as a promising material in regenerative medicine.^[14] In another study, Raghunath *et al.*

* Correspondence to: Nilhan Kayaman-Apohan, Marmara University, Department of Chemistry, 34722 Goztepe-Istanbul, Turkey.
E-mail: napohan@marmara.edu.tr

a B. Oktay, N. Kayaman-Apohan
Department of Chemistry, Marmara University, 34722, Goztepe-Istanbul, Turkey

b S. Erdem-Kuruca, M. Süleymanoğlu
Istanbul Medical Faculty, Department of Physiology, Istanbul University, 34390, Capa-Istanbul, Turkey

showed that the signature biological and physico-chemical properties of collagen are retained in *in vitro* preparations. If the unique properties of triple-helical collagen are desired within the design scaffolds, coating of the scaffolds with collagen is the suitable method.^[15]

Polyvinyl alcohol (PVA) is one of the most important water-soluble, biocompatible, biodegradable, and non-toxic synthetic polymers. Moreover, PVA attracts attention with its good transparency, luster, antielectrostatic properties, chemical resistance, and toughness.^[16] Li *et al.* prepared PVA-based fast dissolving drug carrier nanofiber systems.^[17] In another study, to develop dental scaffolds, PVA-based bio nano-composite fibers were synthesized by electrospinning. Hydroxyapatite nanoparticles (HAp) were added to the PVA solution. The orientation of HAp in the PVA matrix resembled the native mineralized hard tissue.^[18] Applications of electrospun nanofiber mat have been limited because of its dissolubility in various solvents. PVA is readily modified with various cross-linking agents.^[19] Furthermore, as a result of cross-linking, the polymeric nanofiber mat becomes more enduring. Until now, the water insoluble PVA membranes have been generally produced by a two-step process. Firstly, electrospun PVA is produced, and then the membrane is cross-linked *ex situ* by exposure of glutaraldehyde (GA) and a strong acid in solution.^[20] Another approach is to expose the membrane to GA and acid vapors^[21,22] as an alternative to the aforementioned approach. The design of photoreactive and crosslinkable PVA draws considerable interest.^[23,24] PVA is one of the most common biocompatible polymers that can photopolymerise after modification by suitable techniques. Anseth *et al.* used acrylated PVA for cartilage tissue engineering applications.^[25] They demonstrated that the fabricating hydrogels through the copolymerization of polyethylene glycol (PEG) and PVA macromers was an effective tool for encapsulating chondrocytes, controlling gel degradation profiles, and generating cartilaginous tissue. Schmedlen *et al.* investigated the use of photoactive PVA derivatives in the presence of cells and tissues.^[26] They reported the advantages of PVA hydrogel scaffolds over PEG hydrogels, particularly in terms of elastic properties and availability of sites for attachment of bioactive molecules. A number of studies have been performed to fabricate PVA nanofibers for use in tissue engineering. Zhou *et al.*

reported the preparation of the water-soluble chitosan/PVA nanofibers because the trace toxic solvent in electrospun products was harmful to human tissue.^[27] Asran *et al.* demonstrated that the bilayered nanofibers from different PVA/PHB blends could mimic the morphological structure of native ECM of the skin.^[28] In order to more accurately mimic the natural ECM, the researcher has also investigated the electrospinning of natural materials such as collagen. However, these materials often lack the desired physical properties or difficult to electrospun alone. Recently, the degradation behavior of electrospun hydroxyethyl cellulose/PVA and collagen-blended nanofibrous scaffolds was investigated by Zulkifli *et al.*^[29] It was reported that the addition of collagen reduced the degradation rate of the nanofibrous scaffolds, and the scaffolds lost their structural properties over a 12-week *in vitro* degradation. However, in this work, the *in vitro* biocompatibility of the scaffolds was not studied.

The aim of this study was to investigate the use of photopolymerizable PVA nanofiber scaffolds for tissue engineering applications. Collagen was introduced as a bioactive moiety to improve biocompatibility and thus to enhance cell affinity of PVA nanofibers. Methacrylate-modified PVA, as a photo-crosslinkable matrix, was synthesized using glycidyl methacrylate. The resulting polymer was electrospun by a one-step electrospinning approach involving the use of an ultraviolet (UV) lamp for photo-crosslinking. Nanofiber surface was then modified with the collagen. 3T3 and ECV304 cells were homogeneously seeded and cultured onto the scaffolds. Viability and proliferation were measured using methylthiazole tetrazolium assay.

MATERIALS AND METHODS

Materials

Poly(vinyl alcohol) (Mw 146000–186000; 99+% hydrolyzed) and glycidyl methacrylate (97%) were purchased from Sigma Chem. Co. (St. Louis, MO, USA). Hydrochloric acid and itaconic acids ($\geq 99\%$) were provided by Sigma Chem. Co. Irg-819 was supplied by Ciba Specialty Chemicals (Basel, Switzerland). 1,1'-carbonyldiimidazole (CDI) was purchased from Fluka AG (St. Gallen, Switzerland). Collagen (Calf skin) was obtained

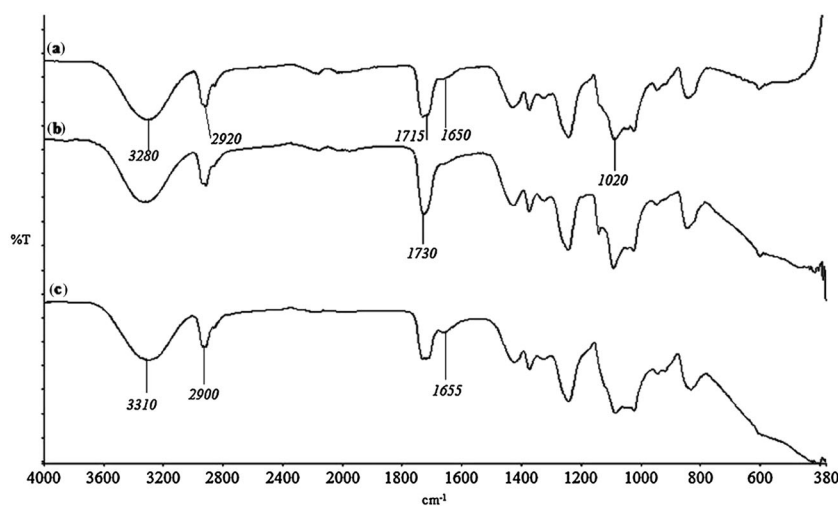


Figure 1. Fourier transform infrared spectroscopy spectra of (a) methacrylated-polyvinyl alcohol (PVA), (b) N-acylimide terminated nanofiber, and (c) collagen-modified PVA nanofiber.

from Calbiochem and used by dissolving in acetic acid (0.1 M). Freshly, double-distilled water was used throughout the experimental work.

Synthesis of methacrylated poly(vinyl alcohol)

Methacrylated PVA was synthesized according to the literature procedure.^[30] Typically, 10 g PVA powder was added in a 250 ml two-necked flask and 90 ml of deionized water was added. The mixture was stirred at 80°C with a magnetic stirrer until a clear solution was formed. After dissolution of PVA, the

system was cooled at room temperature and then excess glycidyl methacrylate was added. pH was adjusted to 1.5 by using hydrochloric acid. The reaction was carried out for 24 hr at room temperature. Once completed, the aqueous solution was poured drop-wise into 250 ml of acetone. The white precipitate was collected by filtration and dried.

Fabrication of nanofibrous scaffold

The nanofibrous web was constructed by electrospinning. For this process, photo-crosslinkable electrospinning solution was

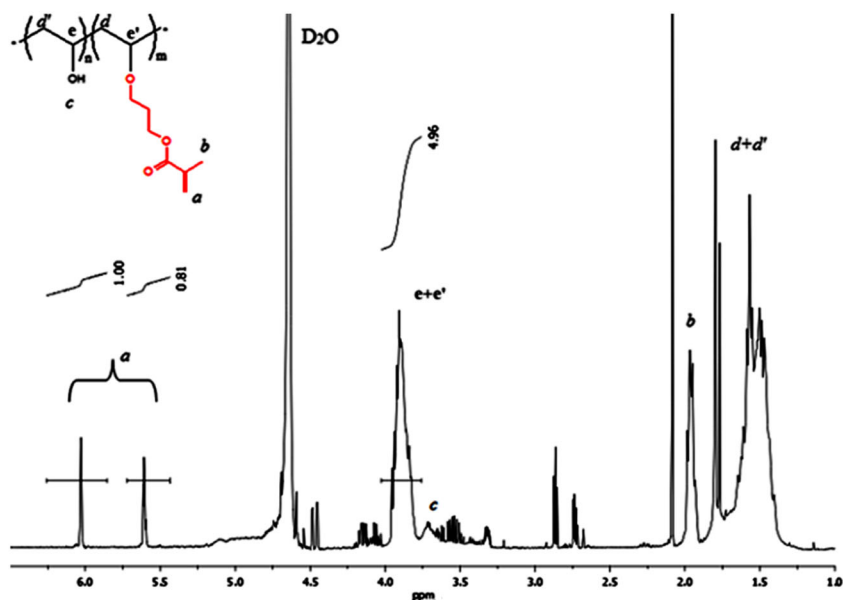


Figure 2. Proton nuclear magnetic resonance spectrum of methacrylated-polyvinyl alcohol in deuterated water. This figure is available in colour online at wileyonlinelibrary.com/journal/pat

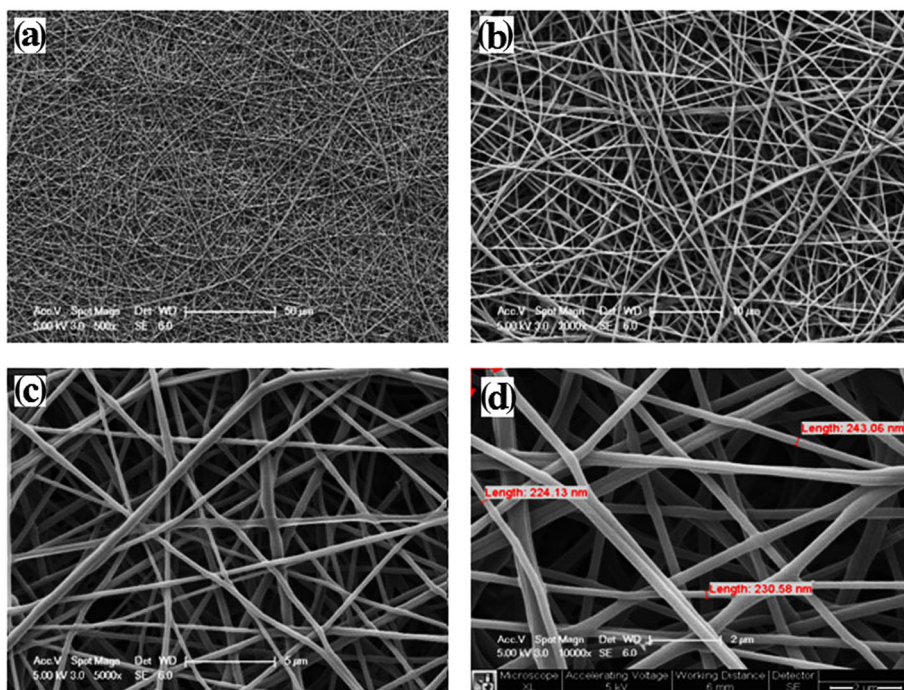


Figure 3. Scanning electron microscopy micrographs of cross-linked polyvinyl alcohol nanofibers (a) 500 \times ; (b) 2000 \times ; (c) 5000 \times magnifications; and (d) in diameter with an average of 220–250 nm. This figure is available in colour online at wileyonlinelibrary.com/journal/pat

prepared. PVA-MA was dissolved in deionized water at 80°C to prepare 10 wt% solution. Itaconic acid (2 wt%), ethylene glycol diacrylate (5 wt%) as cross-linkers, and photoinitiator (Irg-819) (4 wt%) were added to the PVA-MA solution, and the mixture was homogenized. The solution was loaded into a 20 ml syringe fitted with a stainless steel needle and attached to a power supply. Electrospinning parameters were as follows: 26 kV voltage,

constant tip-to-collector distance of 18 cm, and a flow rate of 1 ml/hr. High pressure mercury UV lamp (OSRAM 300W, $\lambda_{\text{max}}=365$ nm) as the UV source was placed inside the electrospinning setup. The polymer solution was collected on rotating cylinder as nanofiber. The obtained nanofiber was carefully detached from the collected surface. The electrospun nanofibers were also thermally post-cured at 140°C for 1 hr. Cross-linking density of the nanofiber increases because of the cross-linking reaction between the hydroxyl groups of PVA and carboxylic acid groups of itaconic acid.^[9]

Preparation of collagen-modified electrospun scaffolds

The surface of the scaffolds was activated by 1,1'-carbonyldiimidazole (CDI). 1.025 g nanofiber was put into a three-necked 50 ml of a round bottom under inert atmosphere. CDI (1.58 g) was dissolved in 10 ml dry tetrahydrofuran, then added to the reaction flask. The reaction mixture was stirred gently at 40°C for 24 hr. The hydroxyl groups of PVA reacted with CDI.^[31] N-Carbonyl imidazol-tethered nanofiber was gently shaken in collagen solution with a concentration of 2 mg/ml acetic acid at room temperature for 24 hr. The product was kept at +4°C.^[32]

Cell seeding on electrospun scaffold for scanning electron microscopy examination

Two types of scaffolds were prepared for cell adhesion and proliferation: collagen-modified and unmodified scaffolds. The same

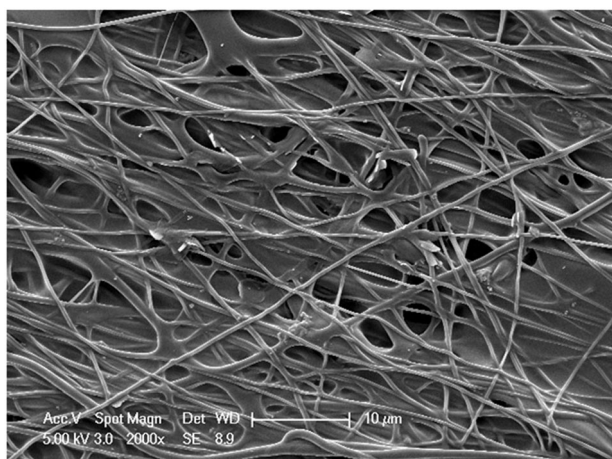


Figure 4. Scanning electron microscopy image of collagen-attached nanofiber.

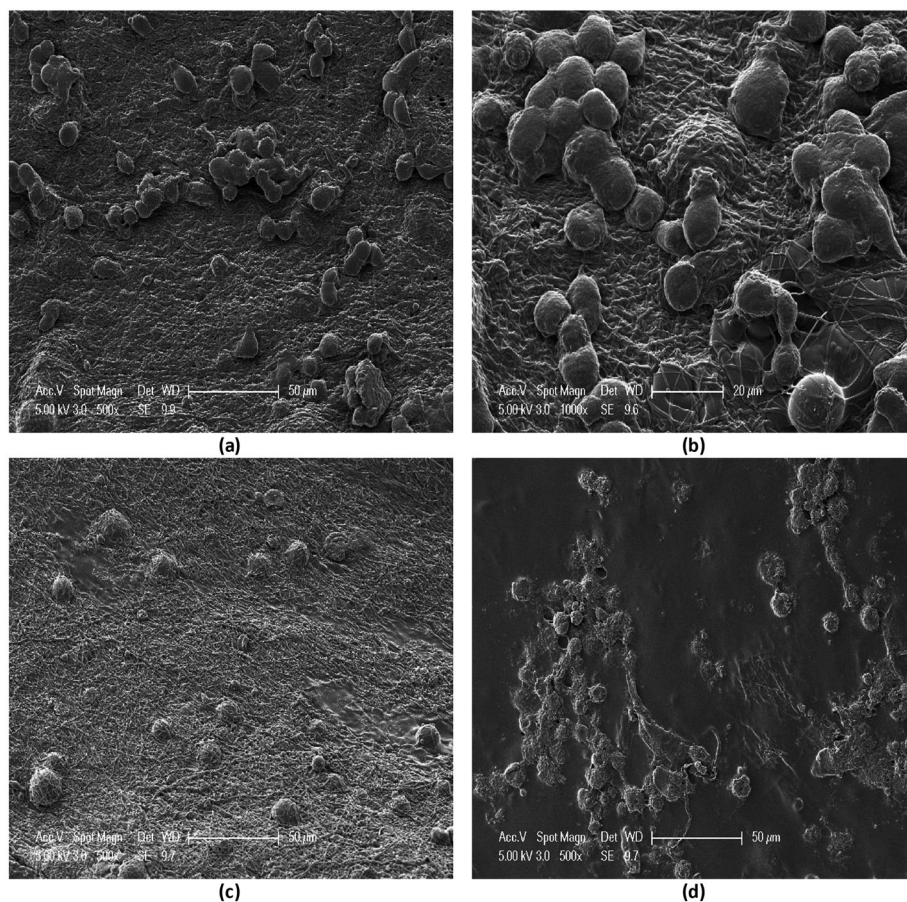


Figure 5. 3T3 cells on the unmodified scaffolds (a) after 2 hr of culture (low-magnification), (b) high-magnification, (c) after 24 hr of culture, and (d) after 72 hr of culture.

procedure was applied to both of the scaffolds. 3T3 mouse fibroblasts and human umbilical vein endothelial cells (ECV304) two cell lines were used for cell culture studies. ECV304 and 3T3 cell lines were obtained from the American Type Culture Collection (ATCC). The cells were cultured in Dulbecco's modified Eagle's medium (Sigma) supplemented with 10% fetal bovine serum (Sigma) and penicillin/streptomycin at 37°C in a 5% CO₂ atmosphere. Once 80% confluency was reached, trypsin (Gibco) was used to harvest the cells and they were diluted to 10⁵ cells/ml. The scaffolds were sterilized in 70% ethanol for 1 hr, and washed three times in sterilized phosphate buffered saline (PBS). Then they were placed in tissue-culture plates for cytotoxicity tests. Cells were seeded on the surface of the fibers at an approximate density of 10⁵ cells/ml. Cell cultures were maintained along 72 hr. After this period, the electrospun scaffolds were taken out from the medium and the cells were then fixed with 2.5% glutaraldehyde. Then, samples were dehydrated in graded series of alcohol (30–100% ethanol in PBS) for 15 min each.

Methylthiazole tetrazolium cytotoxicity assay

Cytotoxic effects of the compounds were evaluated by MTT (3-[4,5-dimethylthiazol-2-yl]-2,5 diphenyltetrazolium bromide) assay, which is reduced by living cells to yield a soluble formazan product using the method of Mossman modified by our laboratory.^[33]

Statistical analysis

Statistical comparison between different scaffolds was carried out using student's *t*-test in a GraphPad Prism program. Differences with *P* < 0.05 were considered statistically significant.

Characterization

Fourier transform infrared (FTIR) spectroscopy was performed on a Perkin Elmer attenuated total reflectance-FTIR spectrophotometer. All FTIR spectra were collected at the range from 4,000 to 400 cm⁻¹. The nuclear magnetic resonance (NMR) spectrum was recorded with 400 MHz Mercury-VX 400 BB model NMR spectrometer in deuterated water. Thermo oxidative stabilities of the PVA and methacrylated PVA were investigated by Perkin-Elmer thermogravimetric analyzer Pyris 1 thermogravimetric analysis (TGA) model (Waltham, MA, USA). The samples were run from 30 to 750°C with a heating rate of 10°C/min under air atmosphere. The morphology of nanofibers was determined by a scanning electron microscopy (SEM) on a Phillips XL 30 field emission gun environmental SEM (FEI Hillsboro, OR, USA). The scaffold samples were stained with 4,6-diamidino-2-phenylindole for cell nuclei staining (Nuclei = blue). Two (xy) and 3-D (xyz) confocal images of the scaffolds were taken with LEICA TCS SPE confocal microscopy.

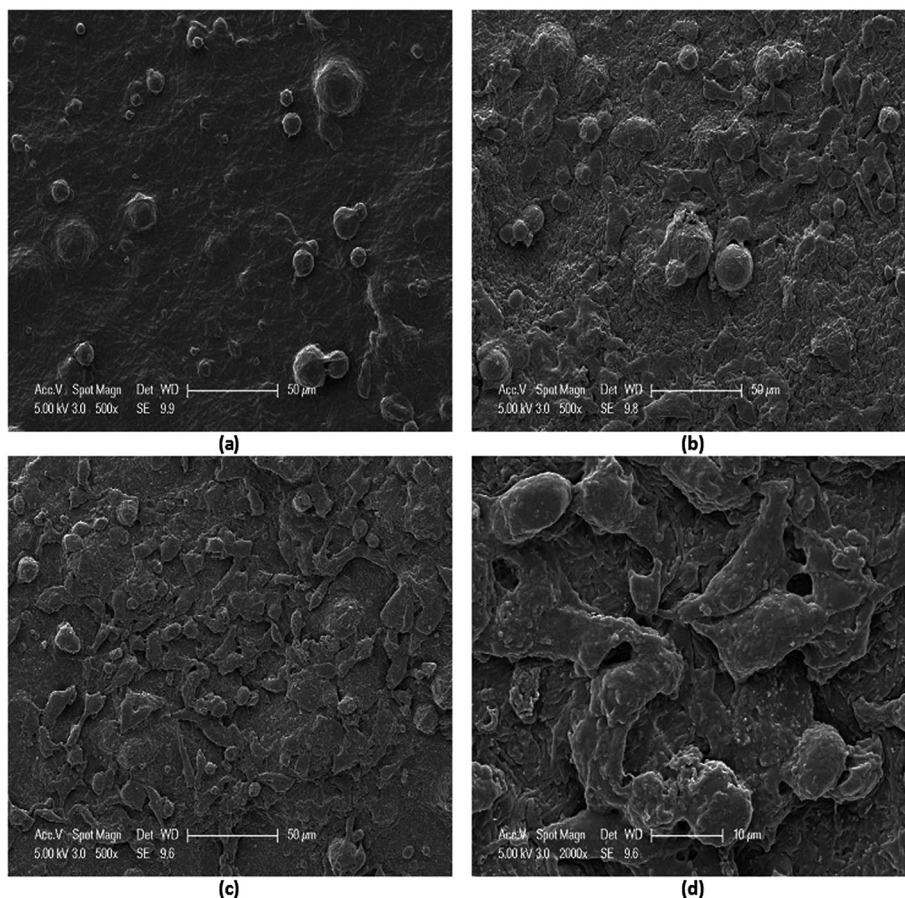


Figure 6. Scanning electron microscopy images of the interaction between 3T3 cells and the collagen-modified scaffold (a) after 2 hr of cell culture, (b) 24 hr, (c) 72 hr (low- magnification), and (d) high-magnification.

RESULTS AND DISCUSSION

Characterization of methacrylated poly(vinyl alcohol)

PVA was modified with glycidyl methacrylate in the presence of acid catalyst. The structure was confirmed by ATR FTIR and $^1\text{H-NMR}$ spectroscopy techniques. FTIR spectrum of the PVA-MA is shown in Fig. 1a. The band at 3280 cm^{-1} is assigned to the characteristic O–H stretching. The characteristic C–H vibrational stretching and C–O vibrational stretching are observed at 2920 cm^{-1} and at 1020 cm^{-1} . Also, the bands at 1650 and 1715 cm^{-1} belong to the methacrylate groups of Glycidyl methacrylate.^[34]

The $^1\text{H-NMR}$ spectrum of PVA-MA is shown in Fig. 2. The $^1\text{H-NMR}$ spectrum of PVA-MA exhibits peaks of chemical shifts of double bond protons (at 5.6–6 ppm) and the unsubstituted methine protons of the PVA backbone (at 3.80–4.1 ppm).^[35,36] Experimental degree of substitution (DS) value of methacrylate groups on PVA backbone was investigated using $^1\text{H-NMR}$. The DS can be calculated from the ratio of the peak areas of the double bond protons to the unsubstituted methine moiety.^[37]

$$\text{Degree of Substitution} = \left(\frac{\text{vinyl protons}}{\text{unsubstituted methine moiety}} \right) * 100 \quad (1)$$

The degree of substitution value of PVA-MA is 18% in deuterated water.

Thermal analysis of methacrylated poly(vinyl alcohol)

The thermal oxidative stability of PVA and PVA-MA was studied by TGA under air atmosphere. In TGA thermograms of PVA and PVA-

MA, a slight weight loss (<5 wt%) was observed at 90°C because of adsorbed moisture inside the polymer.^[38] Both of the TGA curves showed a three-step degradation pattern. The first one ranged from 200 to 350°C with a weight loss of 60%. After which, the second weight loss was observed at temperatures between 350 to 450°C . The first and second weight losses are assumed to be a result of dehydration of the PVA polymer, followed by chain scission. A mass of polyene decomposition yielding low-mass oxygen containing products (such as acetaldehyde, benzaldehyde, and acrolein) and the decomposition of polyene macroradicals to cis and trans derivatives occur in the region.^[39] The final weight loss indicates the decomposition of the polymer backbone due to primary polyenes to cis and trans derivatives followed by their cyclization and the condensation of polyaromatic structures above approximately 450°C .^[40] PVA-MA sample has higher decomposition temperature compared with PVA sample. Moreover, the char yield of PVA-MA at 750°C significantly increased compared with PVA. (from 1% to 4%). The overlay of TGA thermograms of PVA and PVA-MA is given in Supplementary Fig. 1.

Morphological analysis of methacrylated poly(vinyl alcohol)

Fiber diameter and morphology were investigated by SEM analysis. Fig. 3a–d shows SEM micrograph of the cross-linked nanofibers various magnifications. As shown in the SEM micrograph, beadless electrospun fibers with a narrow size distribution were obtained. The nanofibers have an average diameter of about 220–250 nm.

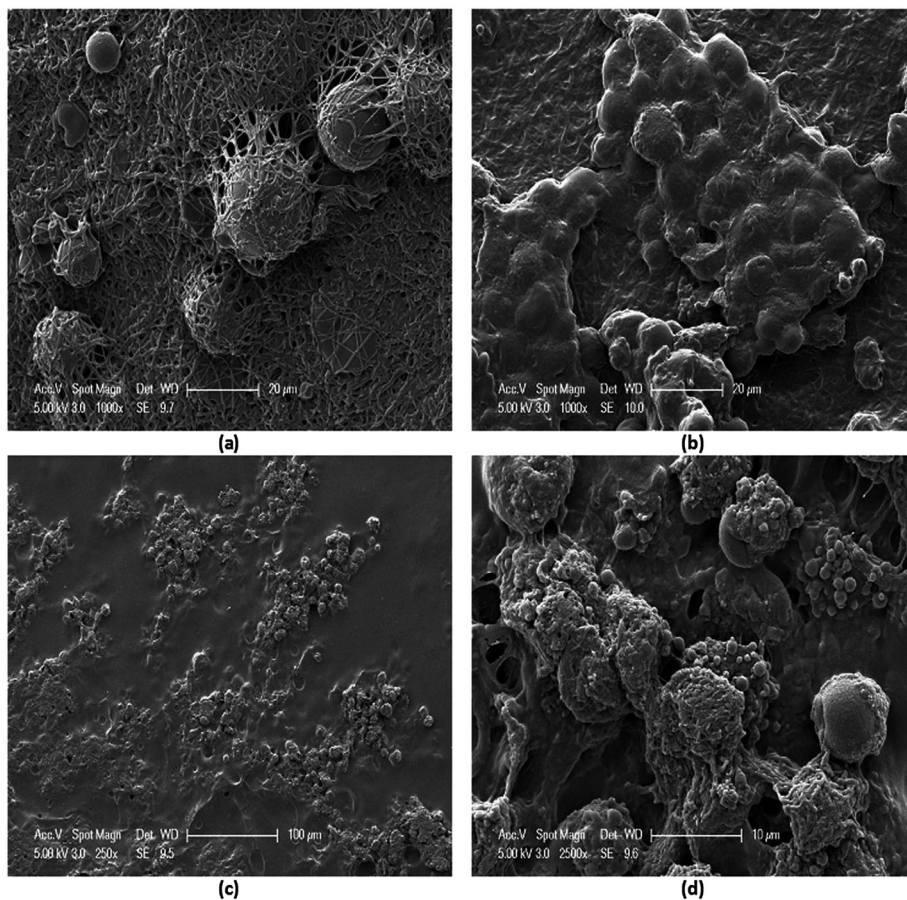


Figure 7. Scanning electron microscopy micrographs of EVC304 cells attached to the unmodified scaffold surface (a) after 2 hr of cell culture, (b) 24 hr, (c) 72 hr low-magnification, and (d) high-magnification.

Modification of electrospun scaffold surface by collagen

Collagen is a natural polymer that is often used for the coupling of amino acids or peptides in tissue engineering. In this study, N-acylimide-terminated electrospun fiber was prepared via the reaction between CDI and the hydroxyl groups. Fig. 1b is the spectrum of the N-acylimide-terminated electrospun fiber. The band appearing at 1730 cm^{-1} was attributed to imidazole group. Collagen was attached to the CDI-activated nanofiber surface. The new peaks were observed in FTIR spectrum of the fiber after collagen modification. As can be seen in Fig. 1c, the characteristic absorbance peaks attributed to collagen; 3310 cm^{-1} (the stretching vibration of N-H group), 1655 cm^{-1} (amide I band from the C=O stretching vibrations coupled to N-H bending vibrations), C-H stretching (2900 cm^{-1}) was monitored for all spectra.^[41,42] Morphology of the collagen modified nanofibers is shown in Fig. 4, in which the nanofibers became collapsed. This may be due to the swelling of nanofiber of PVA in the acidic aqueous solution of collagen during the surface modification process.^[43]

Characterization of the cell seeded electrospun scaffolds

The *in vitro* attachment and growth of 3T3 fibroblast and ECV304 (human umbilical vein endothelial) cells on the electrospun scaffolds were also investigated by SEM. At different times (2, 24, and 72 hr), cells seeded the scaffolds were examined. Fig. 5a and b at two different magnifications indicates that

several cells were present on the scaffold after 2 hr of culture. In Fig. 5c and d, it can be clearly seen that the cells displayed superior spreading on the scaffolds after 24 and 72 hr of cell culture. It is well known that the morphology and cytoskeletal structure of cells changes during adhesion stages (attachment, spreading, migration, and immobilization).^[44–46] It is demonstrated that at the first stage of cell growing, the cells have spherical shapes and then false feet develop. Finally flattened cells form via cell adhesion. It is an indication of a good compatibility.^[47] As can be seen in Fig. 5, the number of the flattened cells is higher than the spherical cells.

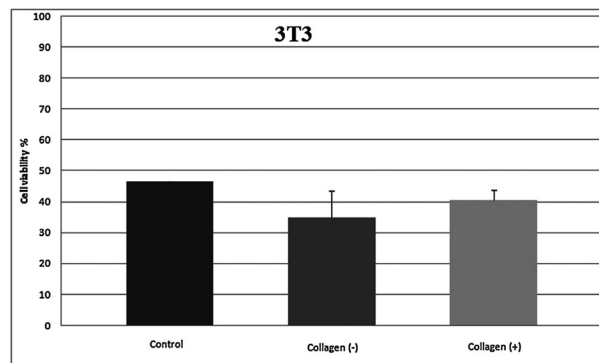


Figure 9. Methylthiazole tetrazolium assay results of proliferation (72 hr) of 3T3 fibroblast cells on the electrospun scaffolds.

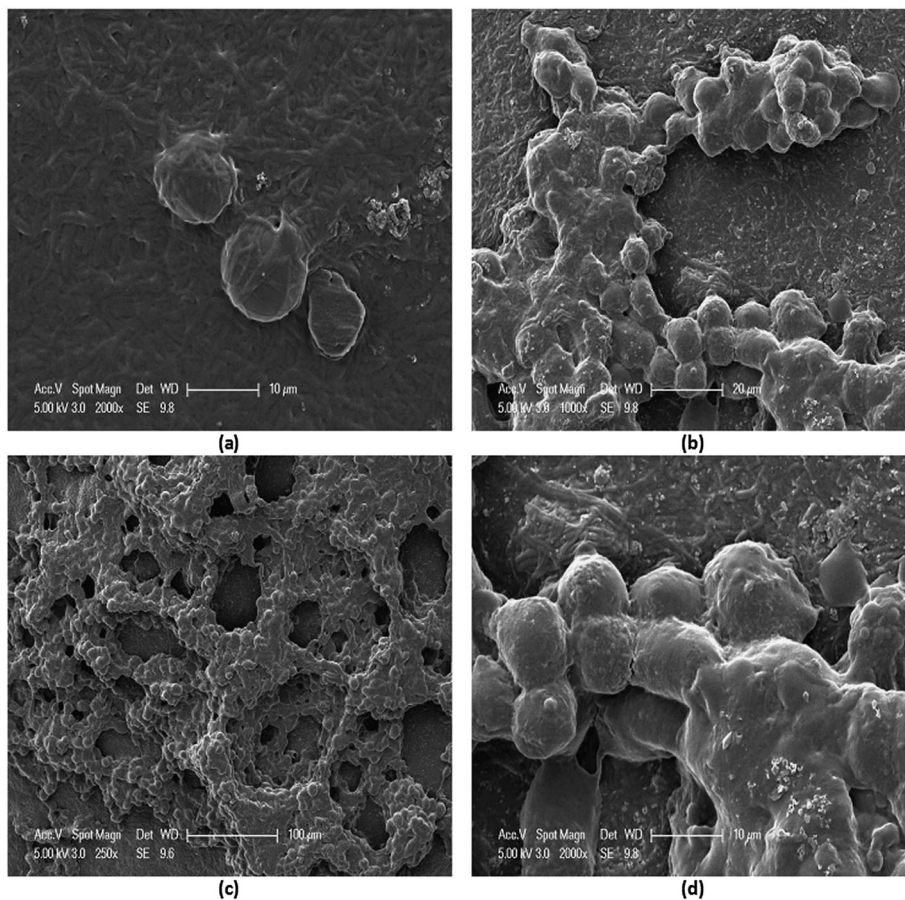


Figure 8. Scanning electron microscopy micrographs of ECV304 cells on the collagen-modified scaffold (a) after 2 hr of cell culture, (b) 24 hr, (c) 72 hr (low-magnification), and (d) high-magnification.

Similarly, SEM images of collagen-modified scaffold (Fig. 6a–d) showed that the fibroblasts grown onto the electrospun scaffold and integrated with the surrounding fibers. However, the morphology of cells was changed and they were more flattened and create connections with each other. The collagen-modified nanofiber scaffolds exhibit excellent support for cell attachment.^[48] It has been reported previously that the adhesion and growth rate of the cells significantly increased when cultured with collagen.^[49]

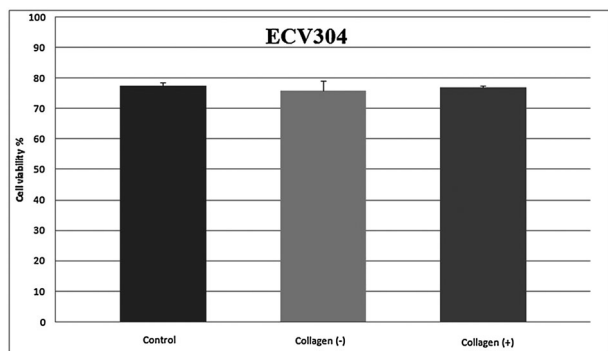


Figure 10. Methylthiazole tetrazolium assay results of proliferation (72 hr) of ECV304 cells on the electrospun scaffolds.

Fig. 7a–d shows SEM images of unmodified scaffold after culture of ECV304 cells. After 2 hr of incubation, it was observed that the cells expanded on the nanofiber scaffold (Fig. 7a). Moreover, it can be seen in Fig. 7b that the cells tend to spread on the nanofiber scaffold with increasing culture time. After 72 hr, the cells covered a large area of the scaffold surface (Fig. 7c and d).

The interaction between the ECV304 cells and collagen modified scaffold is given in Fig. 8. The nanofiber scaffold showed a positive correlation with the ECV304. It can be seen from SEM micrographs that the cells were well-attached to electrospun scaffold. Nanofibrous matrix was completely covered by the cells, and cell proliferation significantly increased after 72 hr of incubation. The rounded morphology gradually changed to a more flattened morphology. This morphology is typically formed by viable cells, which is consistent with the literature.^[50]

We used MTT colorimetric assay to quantitatively evaluate the viability of cells. MTT assay is based on the conversion of MTT insoluble purple formazan crystals by living cells. These formazan crystals are largely impermeable to cell membrane, thus resulting in its accumulation within healthy cells. The number of living cells is directly proportional to the amount of the formazan crystals produced. The color can be quantified spectrophotometrically. After 72 hr in culture, the attachment of the cells on electrospun scaffolds is shown in Figs 9 and 10. It is clear that both of the scaffolds are found biocompatible with 3T3 fibroblast and ECV304 cells, but ECV304 cells showed a higher

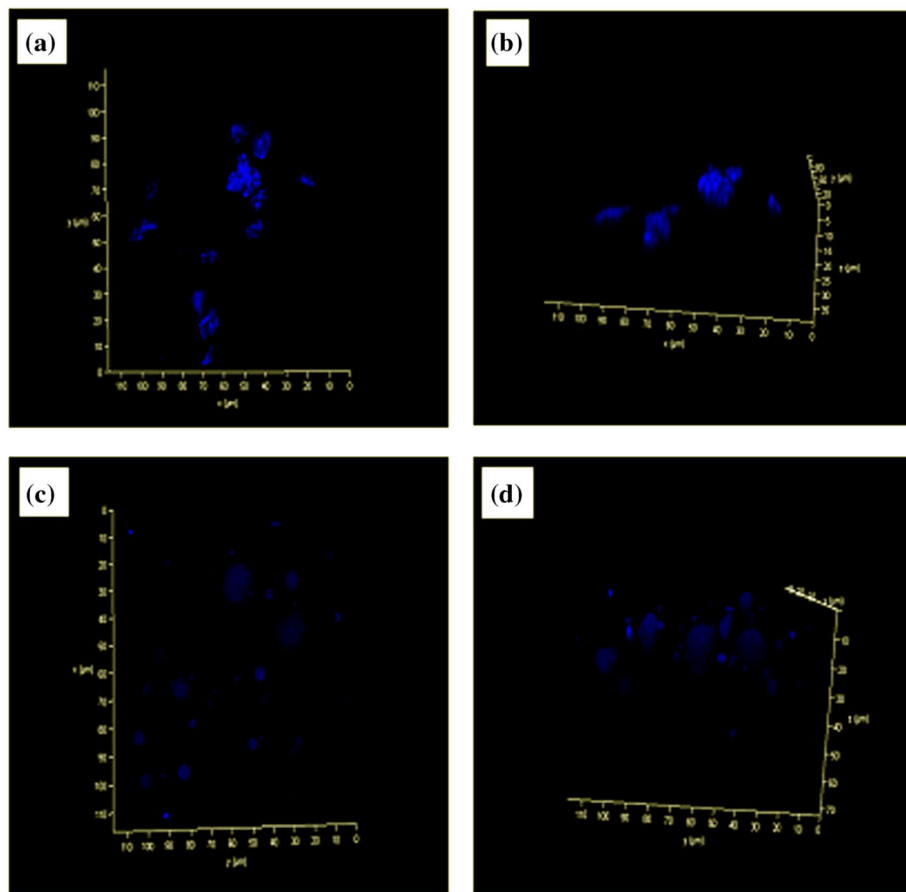


Figure 11. Confocal microscopy images of 3T3 fibroblasts (a) from the surface of the unmodified scaffold and (b) in three (xyz) dimensions, (c) from the surface of the collagen-modified scaffold and (d) from the surface of the collagen-modified scaffold in three (xyz) dimensions. This figure is available in colour online at wileyonlinelibrary.com/journal/pat

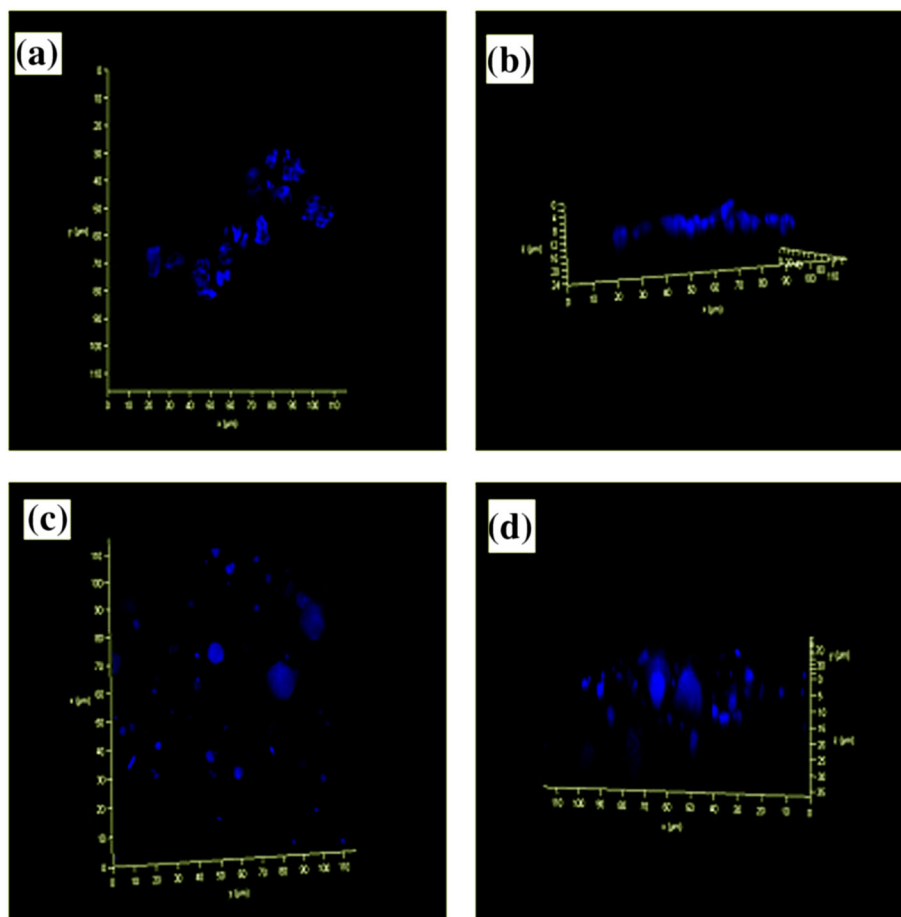


Figure 12. Morphologies of ECV304 cells (a) on the unmodified scaffold in two dimensions (xy) and (b) on the unmodified scaffold in three (xyz) dimensions, (c) on the collagen-modified scaffold in two dimensions (xy) and (d) on the collagen-modified scaffold in three (xyz) dimensions. This figure is available in colour online at wileyonlinelibrary.com/journal/pat

viability. In a previous study, it was reported that the addition of only a small amount of PVA to PHB resulted in a significant decrease in the number of viable dermal fibroblast cells on the nanofibers mats.^[51] However, in this study, we demonstrated that the cell viability of the cross-linked PVA scaffold was very close to collagen-modified PVA scaffold.

Penetration of 3T3 fibroblast and EVC304 cells to the scaffolds was revealed with laser scanning confocal microscopy. Fig. 11a–d shows confocal laser scanning microscopy images of the samples for 3T3 fibroblasts. The z plane indicates the invasion of the cells through the scaffold. 3T3 fibroblasts cells invaded inside the unmodified scaffold at a depth of 15 μm and the collagen modified scaffold at a depth of 20 μm from the surface. Similarly, ECV304 cells showed that the invasion at a depth of 8 μm and 15 μm for unmodified and collagen modified scaffolds, respectively. (Fig. 12a–d)

Miron-Mendoza *et al.* reported the cell motile activity in three-dimensional collagen matrices. It was demonstrated that the cell spreading and migration were dependent on collagen matrix porosity.^[43] Moreover, Misra *et al.* demonstrated that in the case of collagen-modified PCL/gelatin scaffolds, the cell expansion was greater than that of unmodified scaffold. It was clear that cells comply well with the collagen-modified nanofiber surface and were capable of migrating inside the scaffold.^[52] Agudelo-Garcia *et al.* studied the different migratory behavior of glioma cells cultured on aligned and randomly oriented nanofibers. They have

observed a substantial difference in the behavior of glioma cells cultured on aligned nanofibers, where the cells migrate efficiently, versus randomly oriented nanofibers, where migration is highly restricted without evident effects on viability. They have concluded that migration of the cells is regulated by topographical cues of substrate.^[53] In our study, the confocal microscopy results demonstrated that the deeper migration within the collagen-modified nanofiber matrix was achieved because of the specific cell-binding sites of collagen facilitates cell activities.

CONCLUSIONS

We have successfully fabricated homogeneously cross-linked nanofibrous scaffolds by UV combined electrospinning in a single step. Nanofibers were efficiently cross-linked with *in situ* photo cross-linking during electrospinning process to achieve more resistant nanofibers. Two different scaffolds were prepared, and 3T3 fibroblast and ECV304 cells were cultured onto the surfaces. It was demonstrated that the morphology of nanofibrous scaffolds provides a greater surface area for cell attachment and spreading. Cell morphology observations, viability tests, and the migration of cells within the matrix indicate that the collagen-modified nanofibrous scaffolds display better non-cytotoxic behavior and might be a potential candidate for tissue engineering applications.

Acknowledgements

This work was supported by Marmara University, Commission of Scientific Research Project (M.U.BAPKO) under grant FEN-C-DRP-150513-0179

REFERENCES

- [1] C. P. Barnes, S. A. Sell, E. D. Boland, D. G. Simpson, G. L. Bowlin, *Adv Drug Delivery Rev.* **2007**, *59*, 1413–1433.
- [2] M. D. MacArthur, R. O. C. Oreffo, *Nature* **2005**, *433*, 19.
- [3] A. Atala, *J. Tissue Eng. Regen. Med.* **2007**, *1*:83–96.
- [4] Q. P. Pham, U. Sharma, A. G. Mikos, *Biomacromolecules* **2006**, *7*, 2796–2805.
- [5] B. Oktay, E. Baştürk, N. Kayaman-Apohan, M. V. Kahraman, *Polym. Composite* **2013**, *34*, 1321–1324.
- [6] E. Baştürk, M. V. Kahraman, *Polym Composite* **2012**, *33*, 829–837.
- [7] E. Çakmakçı, A. Güngör, N. Kayaman-Apohan, S. Erdem-Kuruca, M. B. Çetin, K. A. Dar, *J. Biomater. Sci. Polym. Ed.* **2012**, *23*, 887–899.
- [8] D. Yang, Y. Li, J. Nie, *Carbohydr. Polym.* **2007**, *69*, 538–543.
- [9] E. Baştürk, S. Demir, Ö. Daniş, M. V. Kahraman, *J. Appl Polym.* **2013**, *127*, 349–355.
- [10] S. Cai, H. Xu, Q. Jiang, Y. Yang, *Langmuir* **2013**, *29*, 2311–2318.
- [11] J. Xue, B. Feng, R. Zheng, Y. Lu, G. Zhou, W. Liu, Y. Cao, Y. Zhang, W. J. Zhang, *Biomaterials* **2013**, *34*, 2624–2631.
- [12] J. A. Matthews, G. E. Wnek, D. G. Simpson, G. L. Bowlin, *Biomacromolecules* **2002**, *3*, 232–238.
- [13] S. Balaji, R. Kumar, R. Sripriya, U. Rao, A. Mandal, P. Kakkar, P. N. Reddy, P. K. Sehgal, *Polym Adv Tech* **2012**, *23*, 500–507.
- [14] M. Kawalec, A. Sitkowska, M. Sobota, A. L. Sieroń, P. Komar, P. Kurcok, *Biomed. Mater.* **2014**, *9*, 065005.
- [15] D. I. Zeugolis, S. T. Khew, E. S. Y. Yew, A. K. Ekaputra, Y. W. Tong, L.-Y. L. Yung, D. W. Huttmacher, C Sheppard, M. Raghunath, **2008**, *Biomaterials* *29*, 2293–2305.
- [16] J. M. Gohil, A. Bhattacharya, P. Ray, *J. Polym. Res.* **2006**, *13*, 161–169.
- [17] X. Li, M. A. Kanjwal, L. Lin, I. S. Chronakis, *Colloids Surf B.* **2013**, *103*, 182–188.
- [18] A. S. Asran, S. Henning, G. H. Michler, *Polymer* **2010**, *51*, 868–876.
- [19] J. H. Lee, U. Lee, K. Jeong, Y. Seo, S. J. Park, H. Y. Kim, *Polym. Int.* **2010**, *59*, 1683–1689.
- [20] D. Puppi, A. M. Piras, N. Detta, H. Ylikauppila, L. Nikkola, N. Ashammakhi, F. Chiellini, *E. Chiellini. J. Bioact. Compat. Pol.* **2011**, *26*, 20–34.
- [21] R. Krishnan, R. Rajeswari, J. Venugopal, S. Sundarrajan, M. Sridhar, S. Ramakrishna, *J. Mater. Sci. Mater. Med.* **2012**, *23*, 1511–1519.
- [22] Y. Wang, Y. L. Hsieh, *J. Membr. Sci.* **2008**, *309*, 73–81.
- [23] J. Xua, X. Lib, F. Sunc, P. Cao, *J. Biomater. Sci. Polym. Ed.* **2010**, *21*, 1023–1038.
- [24] P. J. Martens, T. Holland, K. S. Anseth, *Polymer* **2002**, *43*, 6093–6100.
- [25] P. J. Martens, S. J. Bryant, S. K. Anseth, *Biomacromolecules* **2003**, *4*, 283–292.
- [26] R. H. Schmedlen, K. S. Masters, J. L. Westi, *Biomaterials* **2002**, *23*, 4325–4332.
- [27] Y. Zhou, D. Yang, X. Chen, Q. Xu, F. Lu, J. Nie, *Biomacromolecules* **2008**, *9*, 349–354.
- [28] A. S. Asran, K. Razghandi, N. Aggarwal, G. H. Michler, T. Groth, *Biomacromolecules* **2010**, *11*, 3413–3421.
- [29] F. H. Zulkifli, F. S. J. Hussain, M. S. B. Abdull Rasad, M. M. Yusoff, *Polym. Degrad. Stab.* **2014**, *110*, 473–481.
- [30] P. Martens, K. S. Anseth, *Polymer* **2000**, *41*, 7715–7722.
- [31] Z. S. Akdemir, N. Kayaman-Apohan, M. V. Kahraman, S. Erdem-Kuruca, A. Güngör, S. Karadenizli, *J. Biomater. Sci. Polym. E.* **2011**, *22*, 857–872.
- [32] G. Bayramoğlu, N. Kayaman-Apohan, M. V. Kahraman, S. Karadenizli, S. Erdem-Kuruca, A. Güngör, *Polym. Advan. Technol.* **2012**, *23*, 1403–1413.
- [33] T. Mosmann, *J. Immunol. Methods* **1983**, *65*, 55–63.
- [34] N. Papke, J. Karger-Kocsis, *J. Appl. Polym. Sci.* **1999**, *74*, 2616–2624.
- [35] F. Cavaliere, F. Miano, P. D'Antona, G. Pradossi, *Biomacromolecules* **2004**, *5*, 2439–2446.
- [36] E. G. Crispim, J. F. Piai, A. F. Rubira, E. C. Muniz, *Polym. Test.* **2006**, *25*, 377–383.
- [37] F. Cavaliere, F. Miano, P. D' Antona, G. Pradossi, *Biomacromolecules* **2004**, *5*, 2439–2446.
- [38] P. S. Thomas, J. -P. Guerbois, G. F. Russell, *J. Therm. Ana. Calorim* **2001**, *64*, 501–508.
- [39] H. Yang, S. Xu, L. Jiang, Y. Dan, *J. Macromol. Sci. B* **2012**, *51*:464–480.
- [40] J. W. Gilman, D. L. Vanderhart, T. Kashiwagi, *Proceedings of the American Chemical Society, ACS Symposium series* **1995**, *599*, 161–185.
- [41] S. M. Hashemi, S. Soudi, I. Shabani, M. Naderi, M. Soleimani, *Biomaterials* **2011**, *32*, 7363–7374.
- [42] C. Tangsathakun, S. Kanokpanont, N. Sanchavanakit, T. Banaprasert, S. Damrongsakkul, *J. Met. Mater. Miner.* **2006**, *16*, 37–44.
- [43] M. M. Mendoza, J. Seemann, F. Grinnell, *Biomaterials* **2010**, *31*, 6425–6435.
- [44] S. R. Heidemann, R. E. Buxbaum, *J. Cell Biol.* **1998**, *141*, 1–4.
- [45] M. A. Schwartz, V. Baron, *Curr. Opin. Cell Biol.* **1999**, *11*, 197–202.
- [46] R. A. Stockton, B. S. Jacobson, *Mol. Biol. Cell* **2001**, *12*, 1937–1956.
- [47] M. R. Mohammadi, S. H. Bahramia, M. T. Joghataei, *Mater. Sci. Eng. C Mater. Bio. Appl.* **2013**, *33*, 4935–4943.
- [48] S. Wang, X. Cao, M. Shen, R. Guo, I. Banyai, X. Shi, *Colloids Surf. B.* **2012**, *89*, 254–264.
- [49] Y. M. Hsu, C. N. Chen, J. J. Chiu, S. H. Chang, Y. J. Wang, *J. Biomed. Mater. Res., Part B* **2009**, *91B*, 737–745.
- [50] L. L. Joseph, N. Datta, G. C. Rutledge, *Biomaterials* **2010**, *31*, 491–504.
- [51] A. S. Asran, K. Razghandi, N. Aggarwal, G. H. Michler, T. Groth, *Biomacromolecules* **2010**, *11*, 3413–3421.
- [52] S. Gautam, C. F. Chou, A. K. Dinda, P. D. Potdar, N. C. Mishra, *Mater. Sci. Eng. C Mater. Bio. Appl.* **2014**, *34*, 402–409.
- [53] P. A. Agudelo-Garcia, J. K. De Jesus, S. P. Williams, M. O. Nowicki, E. A. Chiocca, S. Liyanarachchi, P. K. Li, J. J. Lannutti, J. K. Johnson, S. E. Lawler, M. S. Viapiano, *Neoplasia* **2011**, *13*, 831–840.

SUPPORTING INFORMATION

Supporting information may be found in the online version of this paper.